Pharmacological Research 120 (2017) 43–50

Contents lists available at ScienceDirect

Pharmacological Research

journal homepage: www.elsevier.com/locate/yphrs

Breast cancer resistance protein (BCRP/ABCG2) and P-glycoprotein (P-gp/ABCB1) transport afatinib and restrict its oral availability and brain accumulation☆

Stéphanie van Hoppe[a], Rolf W. Sparidans[b], Els Wagenaar[a], Jos H. Beijnen[b], Alfred H. Schinkel[a,*]

[a] Division of Molecular Oncology, The Netherlands Cancer Institute, Amsterdam, The Netherlands
[b] Section of Pharmacoepidemiology & Clinical Pharmacology, Department of Pharmaceutical Sciences, Faculty of Science, Utrecht University, Utrecht, The Netherlands

ARTICLE INFO

Article history:
Received 12 October 2016
Received in revised form
22 December 2016
Accepted 28 January 2017
Available online 10 March 2017

Keywords:
Afatinib
Tyrosine kinase inhibitor
ABCB1
ABCG2
Brain accumulation
Oral availability

ABSTRACT

Afatinib is a highly selective, irreversible inhibitor of EGFR and HER-2. It is orally administered for the treatment of patients with EGFR mutation-positive types of metastatic NSCLC. We investigated whether afatinib is a substrate for the multidrug efflux transporters ABCB1 and ABCG2 and whether these transporters influence oral availability and brain and other tissue accumulation of afatinib.

We used *in vitro* transport assays to assess human (h)ABCB1-, hABCG2- or murine (m)Abcg2-mediated transport of afatinib. To study the single and combined roles of Abcg2 and Abcb1a/1b in oral afatinib disposition, we used appropriate knockout mouse strains.

Afatinib was transported well by hABCB1, hABCG2 and mAbcg2 *in vitro*. Upon oral administration of afatinib, Abcg2$^{-/-}$, Abcb1a/1b$^{-/-}$ and Abcb1a/1b$^{-/-}$;Abcg2$^{-/-}$ mice displayed a 4.2-, 2.4- and 7-fold increased afatinib plasma $AUC_{0\text{-}24}$ compared with wild-type mice. Abcg2-deficient strains also displayed decreased afatinib plasma clearance. At 2 h, relative brain accumulation of afatinib was not significantly altered in the single knockout strains, but 23.8-fold increased in Abcb1a/1b$^{-/-}$;Abcg2$^{-/-}$ mice compared to wild-type mice.

Abcg2 and Abcb1a/1b restrict oral availability and brain accumulation of afatinib. Inhibition of these transporters may therefore be of clinical importance for patients with brain (micro)metastases positioned behind an intact blood-brain barrier.

1. Introduction

ATP-binding cassette (ABC) transporters form a superfamily of transmembrane transport proteins. Two members, ABCB1 (MDR1, P-glycoprotein or P-gp) and ABCG2 (Breast Cancer Resistance Protein, BCRP), are especially important in pharmacokinetics [1,2]. Both affect the disposition of a wide variety of endogenous and exogenous compounds, including many anticancer drugs. They are expressed at pharmacologically important sites such as the apical membranes of enterocytes, hepatocytes and renal tubular epithelial cells, where they can limit gastrointestinal absorption or mediate direct intestinal, hepatic, or renal excretion of their substrates [1,2]. Furthermore, ABCB1 and ABCG2 are expressed on apical membranes of barriers protecting sanctuary tissues such as the blood-brain, blood-placenta and blood-testis barriers, where substrates are pumped directly out of the epithelial or endothelial cells into the blood. Consequently, several chemotherapeutic agents that are ABCB1 and/or ABCG2 substrates have restricted brain accumulation [1–4]. Improving brain accumulation of drugs is of high interest in the clinic due to the fact that current therapies are often inefficient in eradicating brain tumors or brain metastases situated in whole or in part behind an intact blood-brain barrier (BBB) [3,4].

Afatinib (Gilotrif/Giotrif, BIBW 2992) is an orally administered tyrosine kinase inhibitor (TKI) for the treatment of patients with distinct types of metastatic non-small cell lung carcinoma (NSCLC), whose tumor genes have epidermal growth factor receptor (EGFR) exon 19 deletions or exon 21 (L858R) substitution mutations [5].

☆ This work was supported by internal funds within the Netherlands Cancer Institute.

* Corresponding author at: The Netherlands Cancer Institute, Division of Molecular Oncology, Plesmanlaan 121, 1066 CX, Amsterdam, The Netherlands.
E-mail address: a.schinkel@nki.nl (A.H. Schinkel).

http://dx.doi.org/10.1016/j.phrs.2017.01.035
1043-6618/

Approved by the FDA in July 2013, afatinib is a highly selective, irreversible inhibitor of the EGFR and of the human epidermal growth-factor receptor (HER)-2 [6]. It is barely metabolized, with a total recovery percentage of 89.5% of unchanged drug in the urine and feces over 72 h after dosing in humans [7]. Both EGFR and HER-2 are members of the receptor tyrosine kinase (RTK) superfamily [8] and overexpression of both receptors is often found in human cancers such as gliomas, carcinomas of the breast, ovaries, bladder, and lung, including NSCLC. The overexpression, due to gene amplification, is often associated with higher EGFR pathway signaling activity, increased proliferation of cancer cells and reduced apoptosis [9]. It has further been shown preliminarily in cell lines, that afatinib appears effective against a subset of these various cancers overexpressing EGFR and HER-2 [10–12], making it an attractive candidate for further clinical research.

Several published studies indicate that afatinib can interact with ABCB1 and ABCG2 [13–15]. It has for instance been shown that afatinib affects ABCB1 and ABCG2 in several cancer cell lines by blocking substrate transport and/or down-regulating mRNA and protein expression of the transporters [13,15]. However, these same studies reported conflicting data on the ability of afatinib to inhibit ABCB1. FDA and EMA registration information mentions that afatinib is a transported substrate and inhibitor of ABCB1 and ABCG2 [5,16,17], but the limited documentation provided does not allow an assessment of the extent of these processes. In case these efflux transporters can efficiently transport afatinib, this might potentially lead to a decreased accumulation of this drug in target tumors expressing these transporters. Moreover, brain metastases are likely to occur with a subset of cancers, the frequency being highest in lung cancer relative to other common epithelial malignancies [18]. Given the high ABCB1 and ABCG2 expression in the BBB, these transporters could potentially limit afatinib brain accumulation, which might lead to reduced therapeutic efficiency against NSCLC brain metastases. We therefore aimed in this study to investigate whether and to what extent afatinib is transported by one or both of these transporters, and how this might affect oral plasma pharmacokinetics and brain penetration of the drug in Abcb1a/1b and Abcg2 mouse models.

2. Materials and methods

2.1. Chemicals

Afatinib (>99%) was obtained from Alsachim (Illkirch, France). Zosuquidar was purchased from Sequoia Research Products (Pangbourne, UK) and Ko143 was obtained from Tocris Bioscience (Bristol, UK). All chemicals used in the chromatographic afatinib assay were described before [19].

2.2. Transport assays

Polarized Madin-Darby Canine Kidney (MDCKII) cell lines and subclones transduced with either human (h)ABCB1, (h)ABCG2 [20], or mouse (m)Abcg2 cDNA were cultured and used in the transepithelial transport assays as described previously [21]. Transport assays were performed using 12-well Transwell® 3402 plates, 3.0 μm pore size (Corning Inc., USA) in DMEM with 10% fetal bovine serum (FBS). The parental cells and subclones were seeded at a density of 2.5×10^5 cells per well and cultured for 3 days to allow formation of an intact monolayer. Membrane tightness was assessed by measurement of transepithelial electrical resistance (TEER) using reference values that were previously established and well correlated to <1% transepithelial [^{14}C]-inulin leakage per hour [21]. The transepithelial transport experiment was started by pre-incubating the cells with or without the relevant inhibitors during 1 h, thereafter (t = 0) medium in the donor compartments was replaced with complete medium containing 2 μM afatinib alone or in combination with the appropriate inhibitors. In the inhibition experiments, 5 μM zosuquidar (ABCB1 inhibitor) and/or 5 μM Ko143 (ABCG2/Abcg2 inhibitor) were added to both apical and basolateral compartments. Plates were kept at 37 °C in 5% CO_2 during the experiment, and 50-μl aliquots were taken from the acceptor compartment at 2, 4 and 8 h for measurement of afatinib concentrations. Samples were stored at −30 °C for later LC–MS/MS measurement. Total amount of drug transported to the acceptor compartment was calculated after correction for volume loss for each sampling time point. Active transport was expressed by the transport ratio (r), which is defined as the amount of apically directed transport divided by the amount of basolaterally directed transport at a defined time point.

2.3. Animals

Female wild-type, *Abcb1a/1b*$^{-/-}$ [22], Abcg2$^{-/-}$ [23] and Abcg2$^{-/-}$;Abcb1a/1b$^{-/-}$ mice [24], all of a >99% FVB genetic background, were used. Mice between 9 and 14 weeks of age were used in groups of five mice per strain. The mice were kept in a temperature-controlled environment with a 12 h light/12 h dark cycle and received a standard diet (Transbreed, SDS Diets, Technilab – BMI) and acidified water *ad libitum*. Animals were housed and handled according to institutional guidelines in compliance with Dutch and EU legislation.

2.4. Drug solutions and pharmacokinetic experiments

Afatinib was dissolved at a concentration of 20 mg/ml in 50% (v/v) polysorbate 80, 50% (v/v) ethanol. It was then further diluted with 5% (w/v) glucose in water, to obtain a 1 mg/ml afatinib solution in water containing 2.5% (v/v) polysorbate 80, 2.5% (v/v) ethanol, and 4.75% (w/v) glucose. Afatinib was administered orally at a dose of 10 mg/kg (10 μl/g). All working solutions were prepared freshly on the day of the experiment. To minimize variation in absorption, mice were fasted for 3 h prior to oral administration of afatinib using a blunt-ended needle. For the pharmacokinetic experiment, 50-μl blood samples were drawn from the tail vein using heparin-coated capillaries (Sarstedt, Germany) at 0.5, 1, 2, 4 and 8 h or 0.25, 0.5 and 1 h. At 24 h or 2 h, mice were anesthetized using isoflurane and blood was collected via cardiac puncture. Immediately thereafter, mice where sacrificed by cervical dislocation and brain, spleen, liver and kidney were rapidly removed, weighed and subsequently frozen as whole organ at −30 °C. Prior to analysis, organs were allowed to thaw and then homogenized in appropriate volumes (1–3 ml) of 4% (w/v) bovine serum albumin (BSA) in water using a FastPrep® -24 homogenizer (MP-Biomedicals, NY, USA). Homogenates were stored at −30 °C. Blood samples were centrifuged immediately after collection at 9000*g* for 6 min at 4 °C, and plasma was collected and stored at −30 °C until analysis.

2.5. Drug analysis

Afatinib concentrations in culture medium, plasma and tissues were determined with a previously reported liquid chromatography-tandem mass spectrometric (LC–MS/MS) assay for afatinib, with a calibration curve ranging from 0.5 to 500 ng/ml for plasma [19] and tissue homogenates and from 1.5 to 1500 ng/ml for culture medium. Tissue concentrations were calculated correcting for the individual tissue weights, resulting in ng afatinib per gram tissue.

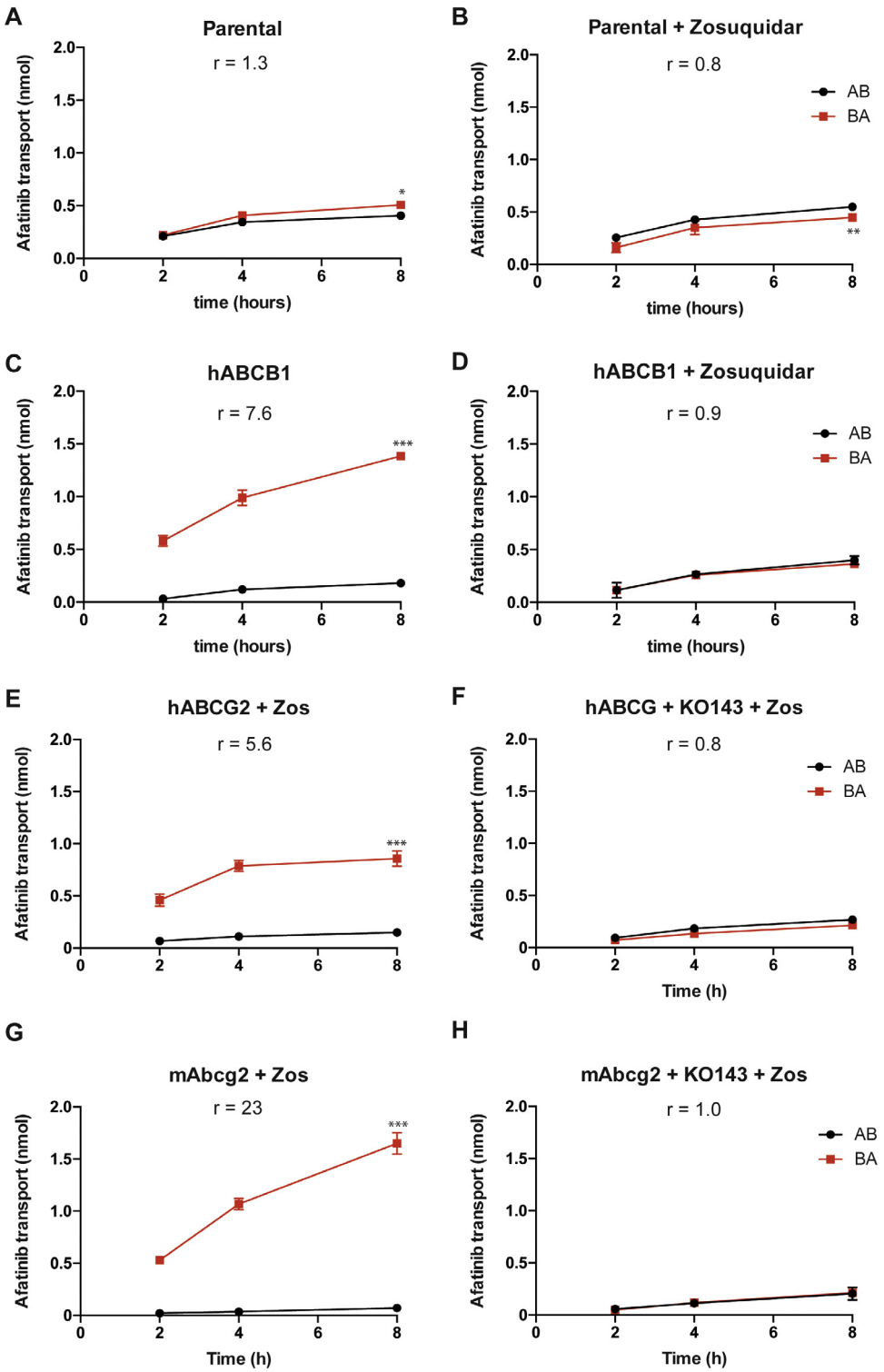

Fig. 1. *In vitro* transport of afatinib. Transepithelial transport of afatinib (2 μM) was assessed in MDCK-II cells either non-transduced (**A, B**) or transduced with hABCB1 (**C, D**), hABCG2 (**E, F**), or mAbcg2 (**G, H**) cDNA. At T = 0 h afatinib was added to the donor compartment; thereafter at t = 2, 4 and 8 h the concentrations were measured and plotted as total amount (nmol) of transport (n = 3). **B, D-H**: Zosuquidar (5 μM) and/or Ko143 (5 μM) were added as indicated to inhibit hABCB1 and hABCG2 or mAbcg2, respectively. *r*, relative transport ratio. Panels E–H: Zos = zosuquidar. BA (red squares) translocation from the basolateral to the apical compartment; AB (black circles), translocation from the apical to the basolateral compartment. Data are presented as the mean ± SD. Owing to high experimental reproducibility, in many cases the error bars are smaller than the symbols used to denote a data point. *, $P < 0.05$; **, $P < 0.01$; ***, $P < 0.001$ compared with AB translocation. (For interpretation of the references to colour in this figure legend, the reader is referred to the web version of this article.)

2.6. Statistical analysis and pharmacokinetic calculations

The unpaired two-tailed Student's *t*-test was used to determine statistical significance for transepithelial transport. In pharmacokinetic experiments, the area under the curve (AUC) of the plasma concentration-time plot was calculated using the trapezoidal rule, without extrapolating to infinity. The maximum drug concentration in plasma (C_{max}) and the time to reach maximum drug

concentration in plasma (T_{max}) were determined directly from individual concentration–time data. The elimination rate constant was calculated with the Microsoft Excel plug in PKsolver [25] with the following formula: $(\ln(y1) - \ln(y2))/(t2 - t1)$. Relative organ accumulation (P_{organ}) was calculated by dividing organ concentrations (C_{organ}) at either t = 2 h or t = 24 h by the area under the plasma concentration-time curve from 0 to 2 h ($AUC_{0\text{-}2h}$) or 0–24 h ($AUC_{0\text{-}24h}$), respectively. One-way analysis of variance (ANOVA) was used to determine significance of differences between groups, after which post-hoc tests with Tukey correction were performed for comparison between individual groups. When variances were not homogeneous, data were log-transformed before statistical tests were applied. Differences were considered statistically significant when $P < 0.05$. Data are presented as means ± SD.

3. Results

3.1. Afatinib is transported by hABCB1, hABCG2 and mAbcg2

We first studied the transport of afatinib *in vitro* by measuring afatinib (2 μM) translocation through polarized monolayers of MDCKII cell lines transduced with human (h)ABCB1, hABCG2 or mouse (m)Abcg2 cDNA. As shown in Fig. 1A, we observed low apically directed afatinib transport in the parental cell line (transport ratio $r = 1.3$). This was somewhat decreased (to an r of 0.8) when adding the ABCB1 inhibitor zosuquidar (Fig. 1B), suggesting that this background transport could be mediated by the low amount of endogenous canine ABCB1 present in the MDCKII cells [26]. In MDCKII cells transduced with hABCB1, we observed extensive apically directed transport with $r = 7.6$, which was completely blocked by zosuquidar ($r = 0.9$, Fig. 1C and D). To suppress any endogenous canine ABCB1 activity, subsequent experiments on ABCG2-mediated transport were done in the presence of zosuquidar. Both hABCG2 and mAbcg2 efficiently transported afatinib in the apical direction ($r = 5.6$ and $r = 23$, respectively) (Fig. 1E and G). This transport was completely abrogated ($r = 0.8$ and $r = 1.0$, respectively) by treatment with the ABCG2 inhibitor Ko143 (Fig. 1F and H). Overall, afatinib appears to be well transported by hABCB1, hABCG2 and mAbcg2.

3.2. Abcg2 and Abcb1 each restrict the oral availability of afatinib in mice

Afatinib is given orally to patients. We therefore started with a pilot experiment with oral afatinib (10 mg/kg) in WT and *Abcb1a/1b;Abcg2*$^{-/-}$ mice, analyzing plasma concentrations and tissue accumulation after 8 h. The results indicated a substantial impact of this combined transporter deficiency on oral availability and brain accumulation of afatinib, with highly increased exposure levels in the knockout strain (Supplemental Figs. 1–3). We therefore studied in more detail the single and combined effects of Abcb1 and Abcg2 deficiencies on afatinib plasma pharmacokinetics and organ accumulation using WT, *Abcg2*$^{-/-}$, *Abcb1a/1b*$^{-/-}$, and *Abcb1a/1b;Abcg2*$^{-/-}$ mice. Plasma exposure of afatinib over 24 h ($AUC_{0\text{-}24}$) was increased by the absence of Abcg2 by 4.2-fold ($P = < 0.001$), by the absence of Abcb1a/1b by 2.4-fold ($P < 0.01$), and by the absence of both Abcg2 and Abcb1a/1b by 7-fold ($P < 0.001$) compared to WT mice (Fig. 2A; Table 1, 24 h data). These results indicate that each of these transporters can substantially affect the intestinal uptake and/or the systemic elimination of afatinib, thus restricting its oral availability. The marked contribution of each of the individual transporters was further supported by comparison of the plasma $AUC_{0\text{-}24}$ values of the single knockout strains with the combination knockout strain (Table 1, 24 h data).

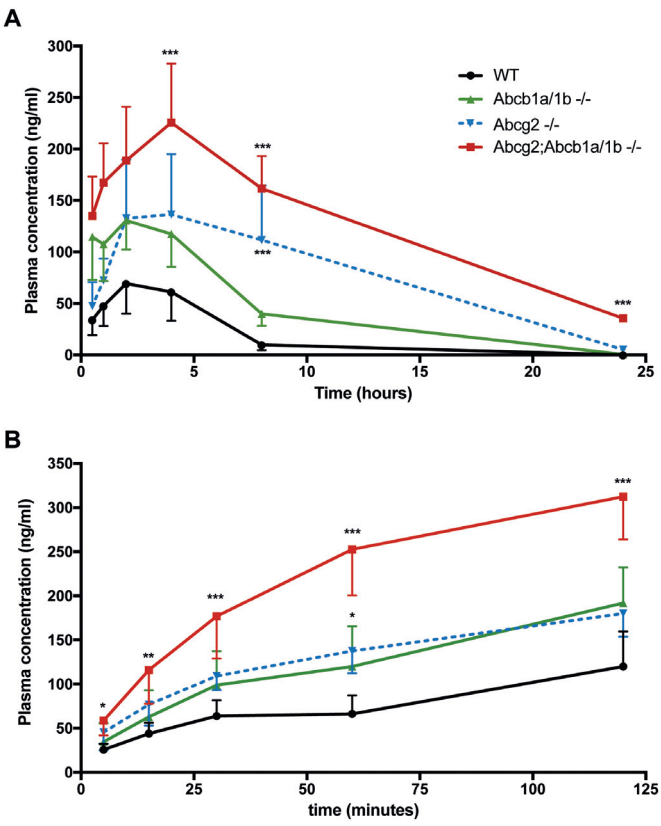

Fig. 2. Plasma concentration-time curves of afatinib in female WT (black squares), *Abcg2*$^{-/-}$ (blue triangles), *Abcb1a/1b*$^{-/-}$ (green triangles), and *Abcg2*$^{-/-}$*;Abcb1a/1b*$^{-/-}$ mice (red squares) over 24 h (**A**) and 120 min (**B**) after oral administration of 10 mg/kg afatinib. Data are given as mean ± SD (SD rendered one-sided for improved clarity). *, $P < 0.05$; **, $P < 0.01$; ***, $P < 0.001$ compared to WT mice. Statistical analysis for the 24 h graph (**A**) for the time points up to 4 h yields $P < 0.001$ at 30 min and 1 h, at 2 h $P < 0.01$ for *Abcg2*$^{-/-}$*;Abcb1a/1b*$^{-/-}$ compared to WT mice. (For interpretation of the references to colour in this figure legend, the reader is referred to the web version of this article.)

Similar results were obtained when measuring the afatinib plasma $AUC_{0\text{-}2}$ in an independent 2-h experiment, with 1.6- and 1.8-fold increased values in *Abcg2*$^{-/-}$ mice and *Abcb1a/1b*$^{-/-}$ mice, respectively ($P < 0.01$ and $P < 0.05$), and a 3-fold increase in the combination knockout strain ($P < 0.001$) compared to the WT mice (Table 1). Like for the 24-h experiment, the contribution of each of the individual transporters yielded significant differences in the $AUC_{0\text{-}2}$ with the combination knockout strain, further supporting that Abcb1 and Abcg2 can each restrict the oral availability of afatinib.

Interestingly, a semi-log plot of the plasma concentrations in the 24-h experiment indicated that, from 8 h on, the plasma clearance in *Abcg2*$^{-/-}$ mice, but especially also in the combination knockout mice, was substantially reduced compared to that in WT and *Abcb1a/1b*$^{-/-}$ mice (Supplemental Fig. 4). This indicates that especially Abcg2 but also Abcb1a/1b can contribute to the plasma clearance of afatinib in mice.

3.3. Abcg2 and Abcb1 each strongly limit afatinib brain accumulation

Tissue concentrations were measured at the last time point of the above-mentioned pharmacokinetic experiments. At 24 h, brain concentrations in *Abcb1a/1b*$^{-/-}$*;Abcg2*$^{-/-}$ mice showed highly significant increases of 1208-fold ($P < 0.001$) compared to WT mice (Fig. 3A; Table 1). The *Abcg2*$^{-/-}$ and *Abcb1a/1b*$^{-/-}$ separate knockout strains also showed a significant increase compared to wild type

Table 1
Pharmacokinetic parameters of afatinib after oral administration of 10 mg/kg to female wild-type, *Abcg2*$^{-/-}$, *Abcb1a/1b*$^{-/-}$, and *Abcb1a/1b*$^{-/-}$;*Abcg2*$^{-/-}$ mice (n = 5–6).

Parameter		Genotype			
	Time (h)	WT	*Abcg2*$^{-/-}$	*Abcb1a/1b*$^{-/-}$	*Abcb1a/1b*$^{-/-}$;*Abcg2*$^{-/-}$
AUC_{0-2} (ng·h/ml)	2	145 ± 33	254 ± 30$^{**,+}$	239 ± 70$^{*,++}$	441 ± 86***
C_{plasma} (ng/ml)		120 ± 40	180 ± 26^{+++}	192 ± 41$^{*,+++}$	312 ± 48***
C_{brain} (ng/g)		51 ± 12	65 ± 16^{+++}	130 ± 66^{+++}	3658 ± 689***
P_{brain} (h^{-1})		0.35 ± 0.06	0.25 ± 0.04^{+++}	0.51 ± 0.15^{+++}	8.34 ± 0.99***
Fold change		1	0.72	1.5	23.8
C_{liver} (μg/g)		10.0 ± 2.9	19.6 ± 4.1*	15.0 ± 6.1^{+}	28.7 ± 10.5***
P_{liver} (h^{-1})		70.7 ± 19	76.7 ± 8.8	63.3 ± 17.2	64.9 ± 20.9
Fold change		1	1.1	0.9	0.9
AUC_{0-24} (ng·h/ml)	24	434 ± 184	1831 ± 651***	1061 ± 253$^{**,++}$	3020 ± 590***
C_{max} (ng/ml)		73.2 ± 31.5	167 ± 39.4*	131 ± 28.3^{+}	227 ± 57.3***
T_{max} (h)		2.8 ± 1.1	4.5 ± 2.5	2	4
C_{brain} (ng/g)		1.7 ± 0.2	7.8 ± 3.7$^{***,+++}$	5.5 ± 1.0$^{***,+++}$	2054 ± 299***
P_{brain} ($*10^{-3}$ h^{-1})		4.3 ± 2.4	4.1 ± 0.9^{+++}	5.4 ± 1.6^{+++}	688 ± 80.1***
Fold change		1	0.95	1.2	160
C_{liver} (ng/g)		12.6 ± 4.8	371 ± 176$^{***,+++}$	22.5 ± 5.1^{+++}	3598 ± 1192***
P_{liver} ($*10^{-3}$ h^{-1})		31.9 ± 15.6	207 ± 110$^{***,+++,\#\#\#}$	21.4 ± 3.6^{+++}	1214 ± 429***
Fold change		1	6.5	0.67	38

AUC, area under the plasma concentration-time curve; Cmax maximum drug concentration in plasma; T_{max}, the time after drug administration needed to reach maximum plasma concentration; C_{brain}, brain concentration; P_{brain}, brain accumulation (C_{brain} divided by plasma AUC); C_{liver}, liver concentration; P_{liver}, liver accumulation (C_{liver} divided by plasma AUC). Note: C_{liver} at 2 h is shown in μg/g and P_{liver} at 24 h is shown in $*10^{-3}$ h^{-1}. *, P < 0.05; **, P < 0.01; ***, P < 0.001 compared to WT mice and $^{+}$, P < 0.05; $^{++}$, P < 0.01; $^{+++}$, P < 0.001 compared to *Abcb1a/1b*$^{(-/-)}$; *Abcg2*$^{(-/-)}$ mice and $^{\#\#\#}$, P < 0.001 compared to *Abcb1a/b*$^{(-/-)}$ mice. Data are given as mean ± SD

mice, although far lower, with increases of 4.6- and 3.2-fold, respectively (P < 0.001). However, as the afatinib plasma concentrations at 24 h were also very different between the strains, this required appropriate correction. Unfortunately, plasma concentrations at 24 h in the WT mice were undetectable, precluding a direct comparison with afatinib brain-to-plasma ratios in the WT mice (Fig. 3B). Correcting the afatinib brain concentrations for the corresponding plasma AUCs resulted in no significant differences in afatinib accumulation in the brains of *Abcg2*$^{-/-}$ and *Abcb1a/1b*$^{-/-}$ mice compared to WT mice (Fig. 3C). However, for *Abcb1a/1b;Abcg2*$^{-/-}$ mice the brain accumulation was 175-fold increased (P < 0.001) compared to that in WT mice, with similar differences observed when compared with *Abcg2*$^{-/-}$ and *Abcb1a/1b*$^{-/-}$ mice (Fig. 3C; Table 1). This indicates that Abcg2 and Abcb1a/1b each by them-

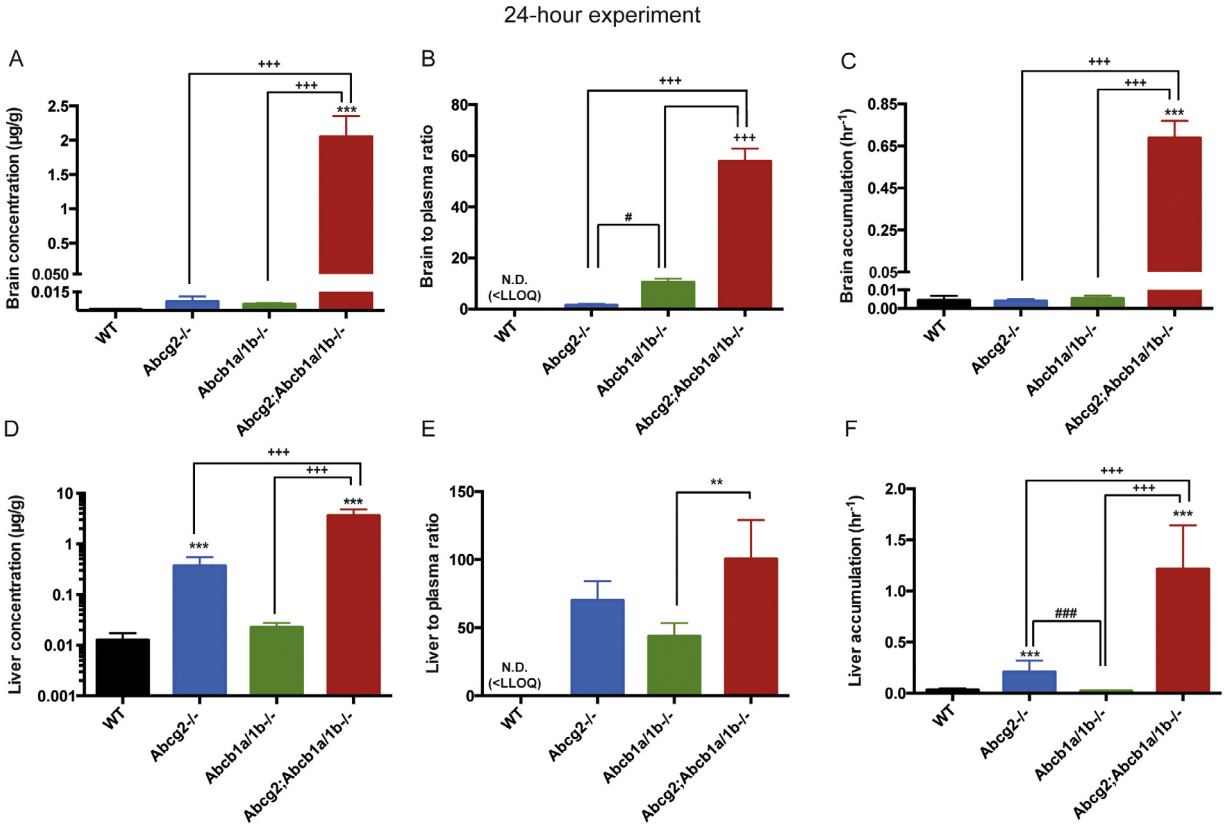

Fig. 3. Brain and liver concentration (**A, D**), tissue-to-plasma ratio (**B, E**) and relative tissue accumulation (**C, F**) of afatinib in female WT, *Abcg2*$^{-/-}$, *Abcb1a/1b*$^{-/-}$ and *Abcg2*$^{-/-}$;*Abcb1a/1b*$^{-/-}$ mice 24 h after oral administration of 10 mg/kg afatinib. Note the log scale used for the liver concentration in panel D. *, P < 0.05; **, P < 0.01; ***, P < 0.001 compared to WT mice and $^{+}$, P < 0.05; $^{++}$, P < 0.01; $^{+++}$, P < 0.001 compared to *Abcb1a/1b*$^{(-/-)}$; *Abcg2*$^{(-/-)}$ mice and $^{\#\#\#}$, P < 0.001 compared to *Abcb1a/b*$^{(-/-)}$ mice. N.D., not detectable; LLOQ, lower limit of quantification 0.5 ng/ml. Data are presented as the mean ± SD.

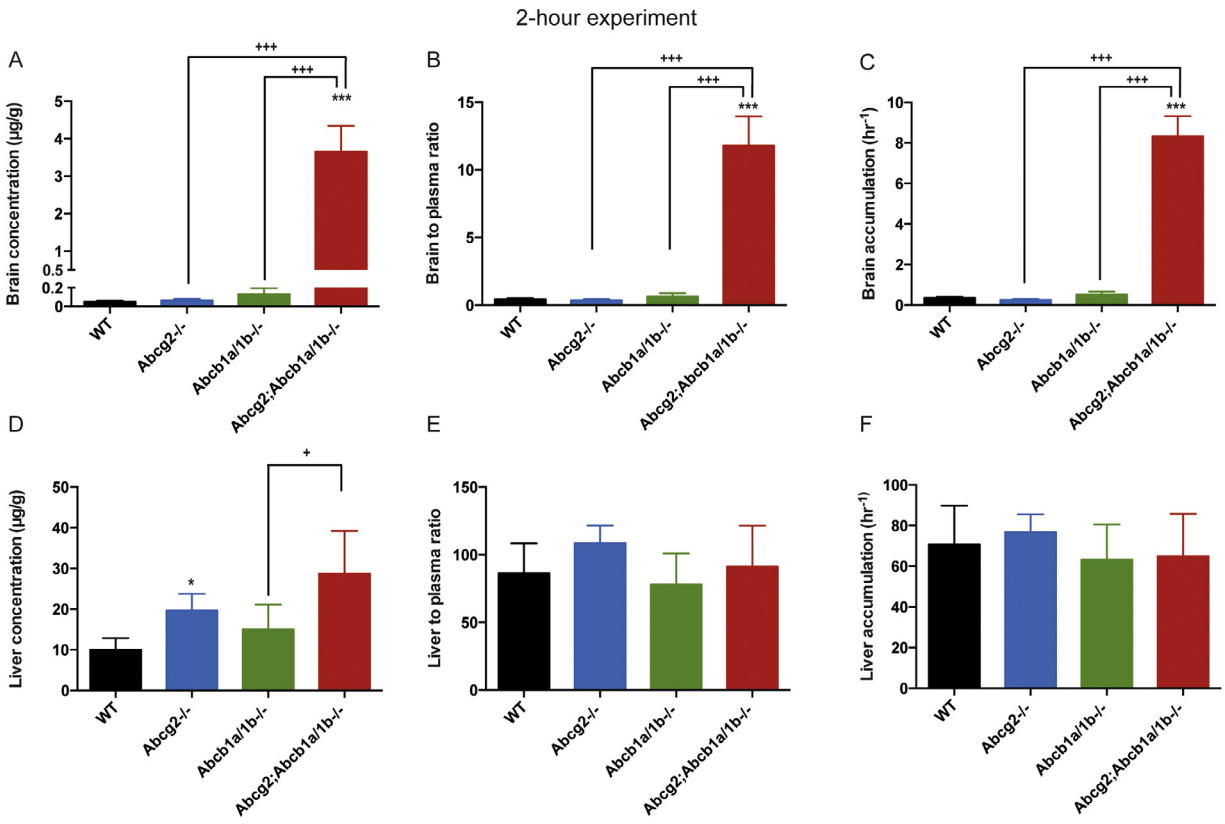

Fig. 4. Brain and liver concentration (**A, D**), tissue-to-plasma ratio (**B, E**) and relative tissue accumulation (**C, F**) of afatinib in female WT, *Abcg2*$^{-/-}$, *Abcb1a/1b*$^{-/-}$ and *Abcg2*$^{-/-}$;*Abcb1a/1b*$^{-/-}$ mice 2 h after oral administration of 10 mg/kg afatinib. *, P < 0.05; **, P < 0.01; ***, P < 0.001 compared to WT mice and $^{+}$, P < 0.05; $^{++}$, P < 0.01; $^{+++}$, P < 0.001 compared to *Abcb1a/1b*$^{(-/-)}$; *Abcg2*$^{(-/-)}$ mice. Data are presented as the mean ± SD.

selves can drastically restrict the brain accumulation of afatinib, and that a combined deficiency of these transporters is needed for a pronounced increase of the brain accumulation of afatinib.

The liver often equilibrates quickly with plasma levels of a drug, which makes it complicated to assess differences between strains when plasma levels are widely divergent (and undetectable in the WT strain), as is the case at 24 h. As shown in Table 1 and Fig. 3D, after oral administration, *Abcg2*$^{-/-}$ mice showed a 29-fold increase (P < 0.001) in liver afatinib concentrations compared to WT mice, whereas *Abcb1a/1b*$^{-/-}$ mice did not show a significant difference compared to the WT mice. With both *Abcb1a/1b* and *Abcg2* knocked out, we observed a more pronounced increase in liver concentration of afatinib compared to WT mice (286-fold, Table 1, Fig. 3D). However, these pronounced differences may well mainly reflect the large differences in plasma afatinib concentration at this time point, as is suggested by the much smaller differences in liver-to-plasma ratios between the strains as far as these could be assessed (Fig. 3E). Rapid equilibration of liver afatinib with plasma afatinib concentrations renders interpretation of a correction for the plasma AUCs (Fig. 3F) problematic, as the strain differences in plasma concentration at 24 h were far greater than the strain differences in plasma AUCs. Similar complications preclude a straightforward interpretation of kidney and spleen parameters at 24 h (Supplemental Fig. 5). Such complications can be circumvented by assessing an earlier time point (e.g., 2 h), where plasma concentration differences are much smaller (see below).

The impact of transporter proteins on tissue accumulation of drugs is especially relevant around the time of maximum plasma concentrations. Mice were therefore sacrificed 2 h after oral administration of 10 mg/kg afatinib. Relative plasma concentrations between the strains up to 2 h were very similar to those seen during the 24 h experiment (Compare Fig. 2A and B). Similar to the results at 24 h after administration, the brain concentration of afatinib in *Abcb1a/1b;Abcg2*$^{-/-}$ mice showed a highly significant 72.4-fold increase (P < 0.001) compared to WT mice. In contrast, no significant differences were found for the single knockout strains compared to WT mice (Fig. 4A, Table 1). Correcting the afatinib brain concentrations for the corresponding plasma concentrations (Fig. 4B) or AUCs (Fig. 4C) yielded similar results. The brain accumulation showed a highly significant, 23.8-fold increase (P < 0.001) for *Abcb1a/1b*$^{-/-}$;*Abcg2*$^{-/-}$ mice compared to WT mice, whereas brain accumulations in the single knockout strains were not significantly different from those in WT (Fig. 4C; Table 1). Thus, also at 2 h, either Abcg2 or Abcb1a/1b alone could profoundly restrict the brain accumulation of afatinib, and only a combined deficiency for both transporters resulted in a drastically increased brain penetration of afatinib.

As explained above, the liver concentration of drugs often equilibrates relatively quickly with the plasma concentration. The data in Fig. 4D–F and Table 1 support that notion for afatinib. Whereas the liver concentration of afatinib was moderately different between the four strains (Fig. 4D), these differences appeared to entirely reflect the plasma concentrations, as both the liver-to-plasma ratios (Fig. 4E) and liver accumulation data (Fig. 4F) showed virtually equal levels between the four strains. Also measurements of these parameters for kidney and spleen (Supplemental Fig. 6) revealed at most modest differences between the strains. Collectively, these data indicate that the profound difference in brain accumulation of afatinib between the strains, especially at 2 h, is a direct consequence of localized activity of Abcg2 and Abcb1a/1b in the blood-brain barrier.

4. Discussion

A number of ABC transporters, including ABCB1 and ABCG2, cause resistance to a wide range of drugs. Expression of some ABC transporters, especially ABCB1 and ABCG2, was found to be associated with resistance to chemotherapy in several cancers, including NSCLC [27,28]. This would suggest the possible importance of inhibiting these transporters when treating patients with chemotherapy to reverse such tumor resistance. Furthermore, NSCLC readily metastasizes to the brain [29], where ABCB1 and ABCG2 are expressed at the blood-brain barrier. Inhibiting both these transporters during chemotherapy could therefore possibly also improve treatment of metastases positioned in part or in whole behind the blood-brain barrier. Afatinib has been approved for the first-line treatment of patients with metastatic NSCLC whose tumors have epidermal growth factor receptor (EGFR) mutations [5,17]. Because the ABC efflux transporters could affect the biological availability of afatinib at several levels, we wanted to investigate the possible effects these transporter proteins might have on afatinib disposition.

We here show that both the ABC efflux transporters ABCG2 and ABCB1 are important factors that can limit uptake of afatinib. We demonstrated that afatinib is efficiently transported by hABCB1, hABCG2 and mAbcg2 *in vitro* (Fig. 1). Similar *in vitro* data were acquired in the past with sunitinib, ceritinib, topotecan and sorafenib [30–32] The plasma afatinib concentrations in the *Abcb1a/1b*$^{-/-}$;*Abcg2*$^{-/-}$ mice were highly increased relative to the WT levels. Single Abcg2 or Abcb1a/1b knockout mice also showed a marked increase in afatinib plasma concentrations, albeit not as high as seen in the combination knockout (Fig. 1). This effect was seen for all the experimental studies at the various end-points of 2, 8 and 24 h after oral administration. These results indicate that the oral availability of afatinib is markedly restricted by both Abcg2 and Abcb1a/1b, which might result from decreased intestinal uptake and/or increased hepatic excretion mediated by these transporters. The results for the single and combination knockout strains suggested roughly additive effects of each transporter in limiting afatinib oral availability. Additionally we found that the plasma clearance was slower in the *Abcb1a/1b*$^{-/-}$;*Abcg2*$^{-/-}$ mice as well as in the *Abcg2*$^{-/-}$ mice, but perhaps less so for *Abcb1a/1b*$^{-/-}$ mice, compared to WT mice (Supplementary Fig. 4). Their mean elimination rate constants were 0.09 h^{-1} ($t_{1/2}$ = 7.6 h), 0.18 h^{-1} ($t_{1/2}$ = 3.8 h), 0.26 h^{-1} ($t_{1/2}$ = 2.7 h) and 0.36 h^{-1} ($t_{1/2}$ = 2.0 h) respectively. However, note that the elimination rate constant for the WT mice was calculated only until 8 h because the 24 h time point was below the quantification limit. Our data indicate that especially Abcg2, but also Abcb1a/1b, directly contribute to the plasma clearance of afatinib in mice.

The accumulation of afatinib was highly increased in the brains of the *Abcb1a/1b*$^{-/-}$;*Abcg2*$^{-/-}$ mice compared to WT mice (Table 1, Figs. 3C, 4C). However, this was not the case for the two single knockout strains. This suggests that in each case the remaining efflux transporter still present at the BBB could virtually completely take over the role of the knocked out transporter. This disproportionate increase in brain accumulation of afatinib observed in the *Abcg2*$^{-/-}$;*Abcb1a/1b*$^{-/-}$ mice compared to the single knockout strains was similar to that found for other TKIs (*e.g.* axitinib, vemurafenib, lapatinib, gefitinib, erlotinib, sunitinib, dasatinib and imatinib [21,30,31,33–37]), and can be explained by relatively straightforward pharmacokinetic models [35,38]. These indicate that, if the two transporters each have a high contribution of efflux transport relative to the background efflux at the BBB in the absence of both transporters, the effect of single transporter ablation on brain accumulation will be far less than the effect of combined ablation. An interesting implication of these models is that, next to Abcg2 and Abcb1a/1b, there can be no other efflux transporters in the BBB that are remotely as efficient in keeping afatinib out of the brain, at least under the conditions we applied.

The liver is pharmacologically a highly important organ; therefore we have also analyzed the accumulation of afatinib in the liver *in vivo*. We show that when the ABCB1 and ABCG2 efflux transporters are knocked out, there is a significant increase in the accumulation of afatinib in the liver (Figs. 3 and 4). However, these changes appear to be driven mainly by the alterations in plasma concentrations between the strains, as suggested by the liver-to-plasma ratios (Fig. 4E; note that the liver-to-plasma ratio in the WT mice at 24 h could not be established because of undetectable plasma levels of afatinib, Fig. 3E).

In previous studies we have found that for some anticancer drugs (everolimus, cabazitaxel) the upregulation of plasma carboxylesterase Ces1c in the ABC transporter knockout strains can affect the pharmacokinetics of these drugs [39,40]. This can occur by strong binding of some drugs to this protein, resulting in pronounced retention of drug in plasma. If this were the case for afatinib, one would expect a substantially decreased liver-to-plasma ratio in the knockout strains, as previously observed for everolimus and cabazitaxel. As there is no indication whatsoever of such a decrease (Fig. 4E), it appears that afatinib is not substantially affected by such a potentially confounding process.

Clinical trials of afatinib up till now have shown positive results in tumor regression in NSCLC patients with EGFR-mutation positive tumors. Progression-free survival in these patients is enhanced in patients without, as well as with brain metastases [41–43]. A phase III trial in patients with second-line recurrent and/or metastatic head and neck squamous cell carcinoma comparing efficacy of afatinib versus methotrexate has shown favorable results for treatment with afatinib, with a higher progression-free survival rate [44]. Thus, although afatinib has been approved for treatment of NSCLC [5,17], it may be beneficial for other tumor types containing the relevant EGFR-mutations as well.

Based on our findings, it is likely that tumors expressing ABCB1 and/or ABCG2 will also demonstrate resistance to afatinib-based chemotherapy. Inhibiting these transporters during afatinib therapy might therefore be beneficial for the response of these tumors. It may further be possible to increase afatinib levels in the brain of patients with CNS involvement for better treatment efficacy when afatinib is coadministered with an efficacious dual inhibitor of ABCB1 and ABCG2 such as elacridar. From our study it appears that this sort of coadministration might perhaps also increase the oral availability and consequently overall tissue levels of afatinib, which should be taken into account for possible dose adjustment, to avoid increased toxicity.

5. Conclusion

Our study shows that ABCG2 and ABCB1 by themselves and together markedly restrict oral availability and brain disposition of afatinib, and mediate its elimination. These results indicate that coadministration of efficacious ABCG2 and ABCB1 inhibitors may increase exposure of afatinib in patients, in transporter-expressing tumors, but especially also in the brain, thus providing an option to better treat NSCLC and its metastases positioned in part or in whole behind a functionally intact blood-brain barrier.

Conflict of interest

The research group of A.H.S. receives revenue from commercial distribution of some of the mouse strains used in this study.

Acknowledgements

We gratefully acknowledge the technical assistance of Levi Buil during the experimental phase, and Cristina Lebre, Changpei Gan, Alejandra Martinez-Chavez, Jing Wang, Xiaozhe Qi and Yaogeng Wang for critical reading of this manuscript.

Appendix A. Supplementary data

Supplementary data associated with this article can be found, in the online version, at http://dx.doi.org/10.1016/j.phrs.2017.01.035.

References

[1] A.H. Schinkel, et al., P-glycoprotein in the blood-brain barrier of mice influences the brain penetration and pharmacological activity of many drugs, J. Clin. Invest. 97 (11) (1996) 2517–2524.
[2] M.L. Vlaming, J.S. Lagas, A.H. Schinkel, Physiological and pharmacological roles of ABCG2 (BCRP): recent findings in Abcg2 knockout mice, Adv. Drug Deliv. Rev. 61 (1) (2009) 14–25.
[3] P.R. Lockman, et al., Heterogeneous blood-tumor barrier permeability determines drug efficacy in experimental brain metastases of breast cancer, Clin. Cancer Res. 16 (23) (2010) 5664–5678.
[4] K.S. Taskar, et al., Lapatinib distribution in HER2 overexpressing experimental brain metastases of breast cancer, Pharm. Res. 29 (3) (2012) 770–781.
[5] U.S. Food and Drug Administration, Approved Drugs: Afatinib. 2013; Available from: http://www.fda.gov/Drugs/InformationOnDrugs/ApprovedDrugs/ucm360574.htm.
[6] D. Li, et al., BIBW2992, an irreversible EGFR/HER2 inhibitor highly effective in preclinical lung cancer models, Oncogene 27 (34) (2008) 4702–4711.
[7] P. Stopfer, et al., Afatinib pharmacokinetics and metabolism after oral administration to healthy male volunteers, Cancer Chemother. Pharmacol. 69 (4) (2012) 1051–1061.
[8] N.E. Hynes, H.A. Lane, ERBB receptors and cancer: the complexity of targeted inhibitors, Nat. Rev. Cancer 5 (5) (2005) 341–354.
[9] Y. Yarden, M.X. Sliwkowski, Untangling the ErbB signalling network, Nat. Rev. Mol. Cell Biol. 2 (2) (2001) 127–137.
[10] A. Di Luca, et al., Label-free LC–MS analysis of HER2+ breast cancer cell line response to HER2 inhibitor treatment, Daru 23 (2015) p40.
[11] Y. Tang, et al., Afatinib inhibits proliferation and invasion and promotes apoptosis of the T24 bladder cancer cell line, Exp. Ther. Med. 9 (5) (2015) 1851–1856.
[12] N. Harbeck, F. Solca, T.C. Gauler, Preclinical and clinical development of afatinib: a focus on breast cancer and squamous cell carcinoma of the head and neck, Future Oncol. 10 (1) (2014) 21–40.
[13] S.Q. Wang, et al., Afatinib reverses multidrug resistance in ovarian cancer via dually inhibiting ATP binding cassette subfamily B member 1, Oncotarget 6 (28) (2015) 26142–26160.
[14] C.H. Chung, et al., A phase I study afatinib/carboplatin/paclitaxel induction chemotherapy followed by standard chemoradiation in HPV-negative or high-risk HPV-positive locally advanced stage III/IVa/IVb head and neck squamous cell carcinoma, Oral Oncol. 53 (2016) 54–59.
[15] X.K. Wang, et al., Afatinib circumvents multidrug resistance via dually inhibiting ATP binding cassette subfamily G member 2 in vitro and in vivo, Oncotarget 5 (23) (2014) 11971–11985.
[16] S. Wind, et al., Clinical pharmacokinetics and pharmacodynamics of afatinib, Clin. Pharmacokinet. 56 (2017) 235–250.
[17] CHMP assessment report: Giotrif. 2013; Available from: http://www.ema.europa.eu/docs/en_GB/document_library/EPAR_-_Public_assessment_report/human/002280/WC500152394.pdf.
[18] L.J. Schouten, et al., Incidence of brain metastases in a cohort of patients with carcinoma of the breast, colon, kidney, and lung and melanoma, Cancer 94 (10) (2002) 2698–2705.
[19] R.W. Sparidans, et al., Liquid chromatography–tandem mass spectrometric assay for the tyrosine kinase inhibitor afatinib in mouse plasma using salting-out liquid–liquid extraction, J. Chromatogr. B Analyt. Technol. Biomed. Life Sci. 1012–1013 (2016) 118–123.
[20] B. Poller, et al., Double-transduced MDCKII cells to study human P-glycoprotein (ABCB1) and breast cancer resistance protein (ABCG2) interplay in drug transport across the blood-brain barrier, Mol. Pharm. 8 (2) (2011) 571–582.
[21] S. Durmus, et al., Oral availability and brain penetration of the B-RAFV600E inhibitor vemurafenib can be enhanced by the P-GLYCOprotein (ABCB1) and breast cancer resistance protein (ABCG2) inhibitor elacridar, Mol. Pharm. 9 (11) (2012) 3236–3245.
[22] A.H. Schinkel, et al., Normal viability and altered pharmacokinetics in mice lacking mdr1-type (drug-transporting) P-glycoproteins, Proc. Natl. Acad. Sci. U. S. A. 94 (8) (1997) 4028–4033.
[23] J.W. Jonker, et al., The breast cancer resistance protein protects against a major chlorophyll-derived dietary phototoxin and protoporphyria, Proc. Natl. Acad. Sci. U. S. A. 99 (24) (2002) 15649–15654.
[24] J.W. Jonker, et al., The breast cancer resistance protein BCRP (ABCG2) concentrates drugs and carcinogenic xenotoxins into milk, Nat. Med. 11 (2) (2005) 127–129.
[25] Y. Zhang, et al., PKSolver: an add-in program for pharmacokinetic and pharmacodynamic data analysis in Microsoft Excel, Comput. Methods Programs Biomed. 99 (3) (2010) 306–314.
[26] L.B. Goh, et al., Endogenous drug transporters in in vitro and in vivo models for the prediction of drug disposition in man, Biochem. Pharmacol. 64 (11) (2002) 1569–1578.
[27] N. Yabuki, et al., Gene amplification and expression in lung cancer cells with acquired paclitaxel resistance, Cancer Genet. Cytogenet. 173 (1) (2007) 1–9.
[28] M. Pesic, et al., Induced resistance in the human non small cell lung carcinoma (NCI-H460) cell line in vitro by anticancer drugs, J. Chemother. 18 (1) (2006) 66–73.
[29] J. Kalifa, et al., Brain metastases from NSCLC: radiation therapy in the era of targeted therapies, J. Thorac. Oncol. 11 (10) (2016) 1627–1643.
[30] B. Poller, et al., Differential impact of P-glycoprotein (ABCB1) and breast cancer resistance protein (ABCG2) on axitinib brain accumulation and oral plasma pharmacokinetics, Drug Metab. Dispos. 39 (5) (2011) 729–735.
[31] S.C. Tang, et al., Brain accumulation of sunitinib is restricted by P-glycoprotein (ABCB1) and breast cancer resistance protein (ABCG2) and can be enhanced by oral elacridar and sunitinib coadministration, Int. J. Cancer 130 (1) (2012) 223–233.
[32] A. Kort, et al., Brain accumulation of the EML4-ALK inhibitor ceritinib is restricted by P-glycoprotein (P-GP/ABCB1) and breast cancer resistance protein (BCRP/ABCG2), Pharmacol. Res. 102 (2015) 200–207.
[33] J.W. Polli, et al., An unexpected synergist role of P-glycoprotein and breast cancer resistance protein on the central nervous system penetration of the tyrosine kinase inhibitor lapatinib (N-{3-chloro-4-[(3-fluorobenzyl)oxy]phenyl}-6-[5-({[2-(methylsulfonyl)ethyl]amino}methyl)-2-furyl]-4-quinazolinamine; GW572016), Drug Metab. Dispos. 37 (2) (2009) 439–442.
[34] S. Agarwal, et al., Distribution of gefitinib to the brain is limited by P-glycoprotein (ABCB1) and breast cancer resistance protein (ABCG2)-mediated active efflux, J. Pharmacol. Exp. Ther. 334 (1) (2010) 147–155.
[35] H. Kodaira, et al., Kinetic analysis of the cooperation of P-glycoprotein (P-gp/Abcb1) and breast cancer resistance protein (Bcrp/Abcg2) in limiting the brain and testis penetration of erlotinib, flavopiridol, and mitoxantrone, J. Pharmacol. Exp. Ther. 333 (3) (2010) 788–796.
[36] J.S. Lagas, et al., Brain accumulation of dasatinib is restricted by P-glycoprotein (ABCB1) and breast cancer resistance protein (ABCG2) and can be enhanced by elacridar treatment, Clin. Cancer Res. 15 (7) (2009) 2344–2351.
[37] R.L. Oostendorp, et al., The effect of P-gp (Mdr1a/1b) BCRP (Bcrp1) and P-gp/BCRP inhibitors on the in vivo absorption, distribution, metabolism and excretion of imatinib, Invest. New Drugs 27 (1) (2009) 31–40.
[38] J.C. Kalvass, G.M. Pollack, Kinetic considerations for the quantitative assessment of efflux activity and inhibition: implications for understanding and predicting the effects of efflux inhibition, Pharm. Res. 24 (2) (2007) 265–276.
[39] S.C. Tang, et al., P-glycoprotein CYP3A, and plasma carboxylesterase determine brain and blood disposition of the mTOR Inhibitor everolimus (Afinitor) in mice, Clin. Cancer Res. 20 (12) (2014) 3133–3145.
[40] S.C. Tang, et al., P-glycoprotein CYP3A, and plasma carboxylesterase determine brain disposition and oral availability of the novel taxane cabazitaxel (Jevtana) in mice, Mol. Pharm. 12 (10) (2015) 3714–3723.
[41] M. Schuler, et al., Afatinib beyond progression in patients with non-small-cell lung cancer following chemotherapy, erlotinib/gefitinib and afatinib: phase III randomized LUX-Lung 5 trial, Ann. Oncol. 27 (3) (2016) 417–423.
[42] M. Hochmair, S. Holzer, O.C. Burghuber, Complete remissions in afatinib-treated non-small-cell lung cancer patients with symptomatic brain metastases, Anticancer Drugs 27 (9) (2016) 914–915.
[43] P. Hoffknecht, et al., Efficacy of the irreversible ErbB family blocker afatinib in epidermal growth factor receptor (EGFR) tyrosine kinase inhibitor (TKI)-pretreated non-small-cell lung cancer patients with brain metastases or leptomeningeal disease, J. Thorac. Oncol. 10 (1) (2015) 156–163.
[44] P.M. Clement, et al., Afatinib versus methotrexate in older patients with second-line recurrent and/or metastatic head and neck squamous cell carcinoma: subgroup analysis of the LUX-Head & Neck 1 trial, Ann. Oncol. 27 (8) (2016) 1585–1593.